

Non-local Magnetic Field-tuned Quantum Criticality in Cubic $\text{CeIn}_{3-x}\text{Sn}_x$ ($x = 0.25$)

A. V. Silhanek,¹ Takao Ebihara,² N. Harrison,¹ M. Jaime,¹ Koji Tezuka², V. Fanelli,¹, and C. D. Batista,¹

¹*National High Magnetic Field Laboratory, Los Alamos National Laboratory, MS E536, Los Alamos, NM 87545, USA*

²*Department of Physics, Shizuoka University, Shizuoka 422-8529, Japan*

(Dated: March 5, 2018)

We show that antiferromagnetism in lightly ($\approx 8\%$) Sn-doped CeIn_3 terminates at a critical field $\mu_0 H_c = 42 \pm 2$ T. Electrical transport and thermodynamic measurements reveal that the effective mass m^* does not diverge, suggesting that cubic CeIn_3 is representative of a critical spin-density wave (SDW) scenario, unlike the local quantum critical points reported in lower-symmetry systems such as $\text{CeCu}_{6-x}\text{Au}_x$ and $\text{YbRh}_2\text{Si}_{2-x}\text{Ge}_x$. The existence of a maximum in m^* at a lower field $\mu_0 H_x = 30 \pm 1$ T may be interpreted as a field-induced crossover from local moment to SDW behavior as the magnitude of the antiferromagnetic order parameter falls below the Fermi bandwidth.

When the Neel temperature of an antiferromagnet is tuned to absolute zero at a quantum critical point (QCP), the uncertainty principle leads to a divergence in the characteristic lengthscale of the fluctuations of the staggered-moment order parameter Ψ [1]. In itinerant d - or f -electron antiferromagnets, strong on-site correlations often cause the renormalized Fermi bandwidth $k_B T^*$ to become comparable to the Neel temperature T_N . A potential locally critical scenario arises in which the extent to which the d - or f -electrons *locally* contribute charge degrees of freedom to the Fermi liquid becomes subject to fluctuations at the QCP [2, 3]. Their effective localization is conditional upon the inequality $T_N > T^*$ being satisfied [4], necessitating $T^* \rightarrow 0$ at the QCP as depicted in Fig. 1a. Several f -electron antiferromagnets, including $\text{CeCu}_{6-x}\text{Au}_x$ [3, 5], $\text{YbRh}_2\text{Si}_{2-x}\text{Ge}_x$ [6] and CeRhIn_5 [7], appear to provide examples of such behavior as function of pressure p , magnetic field H or chemical substitution x . However, no experiment has yet been able to gauge the extent to which local criticality requires the spin fluctuations to be two-dimensional (2D) [2, 3]. Were this an absolute requirement, the unambiguously three-dimensional (3D) spin fluctuation spectrum of cubic CeIn_3 should then provide the essential f -electron counterexample to local criticality [2, 8]. In such a case, one might expect a quantum critical spin-density wave (SDW) scenario to prevail [9] in which T^* remains finite at the QCP as depicted in Fig. 1b.

In spite of CeIn_3 being one of the two original f -electron antiferromagnets in which non-Fermi liquid behavior and superconductivity were reported together under pressure [10], the comparatively large Neel temperature ($T_N \approx 10$ K) requires rather extreme experimental conditions for its complete suppression; i.e. $p_c \approx 25$ kbar and $\mu_0 H_c \approx 61$ T [11]. Neither the steep gradient $\partial T_N / \partial p$ at large p [10] nor the use of pulsed magnetic fields for $\mu_0 H > 45$ T are amenable to precision tuning of the temperature dependent electrical resistivity $\rho(T)$ or direct measurements of the specific heat $C_p(T)$. Prior studies [10, 12, 13] had therefore been unable to determine the applicable scheme in Fig. 1.

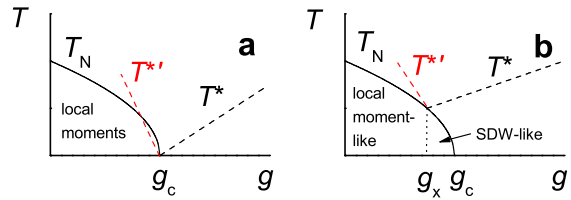


FIG. 1: Schematic of antiferromagnetic quantum criticality tuned at $g = g_c$ according to (a) the locally critical scenario and (b) the SDW scenario, where T represents the temperature scale respectively. The dotted line at g_x in (b) separates regions where the antiferromagnetism is predominantly local moment-like and SDW-like. The parameter g can correspond to p , H or x , depending on the system.

In this paper, we utilize the fact that Sn-substitution of only $\sim 8\%$ of the In sites in CeIn_3 (yielding $\text{CeIn}_{2.75}\text{Sn}_{0.25}$) reduces T_N to ≈ 6.4 K [14, 15] so as to enable quantum criticality of the same type II antiferromagnetic phase as in pure CeIn_3 to be tuned by static magnetic fields $\mu_0 H \leq 45$ T. This also enables us to avoid the technical difficulties associated with performing $C_p(T)$ and magnetization $M_z(H)$ measurements in combined high pressure, strong magnetic field conditions. Sn modifies the electronic structure by reducing the separation between the Fermi energy and the core $4f$ -electron level, pushing this system further towards mixed valence [16]. Prior measurements on single crystalline pure CeIn_3 had shown $T_N(H)$ to be independent of the orientation of H , enabling the use of polycrystalline samples. Polycrystalline $\text{CeIn}_{3-x}\text{Sn}_x$ buttons with concentrations $0 < x < 0.75$ are prepared by arc melting the appropriate quantities of 99.9, 99.999 and 99.9999 % pure Ce, Sn and In respectively, with 5 further arc melts performed after flipping the button between melts for the purposes of homogenization. Samples cut from this button have $\rho(T)$ and $C_p(T)$ behaviors reproducing those obtained by Pedrazzini *et al.* [14]. In-situ $C_p(T)$ and $\rho(T)$

measurements on well characterized samples are then extended to fields $\mu_0 H \leq 45$ T at temperatures $T \gtrsim 1.5$ K.

Figure 2 shows the T, H phase diagram of $\text{CeIn}_{2.75}\text{Sn}_{0.25}$ extracted from the raw $C_p(T)/T$ and $\rho(T)$ data presented in Figs. 3a and b respectively. The transition at T_N corresponds to a minimum in $\partial(C_p(T)/T)/\partial T$ (\circ symbols), which can be further identified with a minimum in $\partial\rho(T)/\partial T$ in Fig. 3c (\square symbols) for $\mu_0 H \lesssim 30$ T. An empirical fit of $T_N = T_{N,0}(1 - (H/H_c)^2)$ to the \circ and \square data points in Fig. 2a yields $\mu_0 H_c = 42 \pm 2$ T. The presence of an anomaly in $C_p(T)/T$ at 35 T and its absence at 45 T are consistent with the above estimate for H_c . Several factors make the present data set consistent with the transition remaining of 2nd order as $H \rightarrow H_c$. These include the vanishing magnitude of the anomaly in $C_p(T)/T$ in Fig. 3a, the absence of a jump in the uniform magnetization $M_z(H)$ at 450 mK in Fig. 3d and the rather shallow slope $\partial T_N/\partial H$ of the phase boundary in Fig. 2 such that $H_c \partial T_N/\partial H \ll p_c \partial T_N/\partial p$ [11].

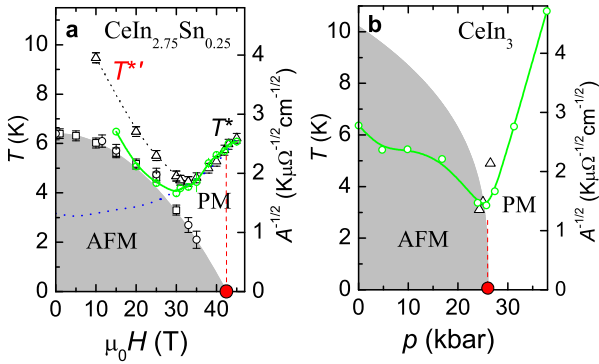


FIG. 2: (a) T, H phase diagram of $\text{CeIn}_{2.75}\text{Sn}_{0.25}$ extracted from $C_p(T)$ (\circ symbols) and $\rho(T)$ data (\square symbols) as described in the text, with the grey region represents the antiferromagnetic (AFM) phase under the fitted $T_N = T_{N,0}(1 - (H/H_c)^2)$ curve. \triangle symbols delineate maxima in $\partial\rho/\partial T$ which are approximately representative of the Fermi bandwidth T^* in the paramagnetic (PM) region. Green circles represent $A^{-1/2}$ in the low temperature limit $T \ll T^*$. The red dashed line represents H_c , while the blue dotted line is $1/\chi' = \partial H/\partial M$ approximately determined from $M_z(H)$ after smoothing and rescaling. All other lines are spline fits between data points. (b) The equivalent phase diagram versus p instead of H using the available data of Knebel *et al.* [12]. Here the \triangle symbols represent T^* after Kawasaki *et al.* [13]

The limiting value of $C_p(T)/T$ as $T \rightarrow 0$ provides an estimate of the coefficient γ that accounts for the electronic contribution γT to $C_p(T)$. It is immediately apparent from the raw $C_p(T)/T$ data shown in Fig. 3a that, in agreement with the SDW scenario for a 3D system [9], γ does not exhibit any obvious signs of an emerging logarithmic divergence at or near H_c . This is in stark con-

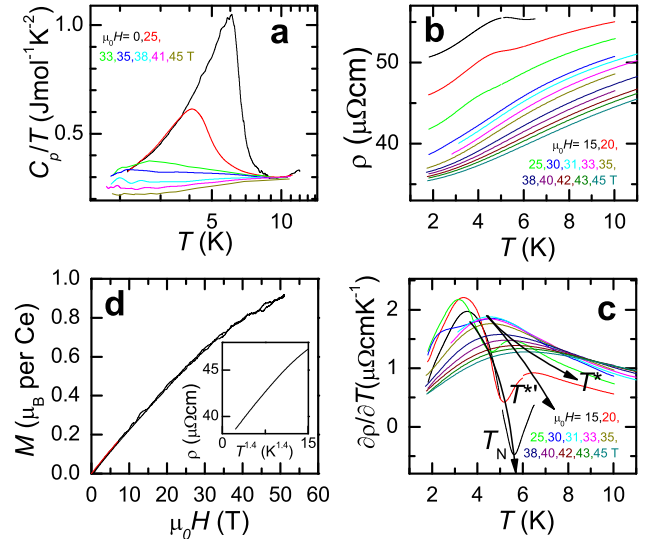


FIG. 3: (a) $C_p(T)/T$ raw data at selected magnetic fields H . (b) $\rho(T)$ data at selected magnetic fields. (c) The differential resistivity $\partial\rho(T)/\partial T$ obtained after polynomial smoothing the raw $\rho(T)$ data. (d) Magnetization of $\text{CeIn}_{2.75}\text{Sn}_{0.75}$ at 450 mK. The inset shows $\rho(T)$ at 30 T plotted versus $T^{1.4}$.

trast to the case of the H -tuned QCPs in $\text{CeCu}_{6-x}\text{Au}_x$ [5] and $\text{YbRh}_2\text{Si}_{2-x}\text{Ge}_x$ [6]. The present findings are nevertheless consistent with the absence of a divergence in $m^*(H, p)$ obtained from p -and H -dependent dHvA experiments on pure CeIn_3 for $\mathbf{H} \parallel < 100 >$ [11, 17, 18].

The electrical transport measurements presented in Fig. 3b further support the absence of a divergence at H_c . Its derivative $\partial\rho(T)/\partial T$ shown in Fig. 3c yields a maximum at T^* (or $T^{*'} \approx 30$ T for $\mu_0 H < 30$ T) plotted in Fig. 2a and an approximately linear region ($\approx 2AT$ where $A \propto m^{*2}$) for $T \lesssim T^*$ over which the Fermi liquid behavior $\rho = \rho_0 + AT^2$ appears to hold [19] (a possible exception being at ≈ 30 T; see Fig. 3d inset and Fig. 4a). On fitting $\rho = \rho_0 + AT^2$ to these $T \lesssim T^*$ regions, $A(H > H_c)$ (solid circles) in Fig. 4a can be seen to exhibit a qualitatively similar behavior to $A(p > p_c)$ in Fig. 4b measured by Knebel *et al.* [12]. In order to understand how the Fermi liquid develops as $H \rightarrow H_c$ and $p \rightarrow p_c$, it is instructive to plot $A^{-1/2}(H, p) \propto 1/m^*$ in Fig. 2. This can be seen to scale with $T^*(H)$ for $H > H_c$, as observed within the paramagnetic regime of other materials [6, 20] implying that T^* approximately corresponds to the Fermi bandwidth. Both $A^{-1/2}(H)$ and $T^*(H)$ also scale with $1/\chi'(H)$ for $H > H_c$ in Fig. 2a, indicating that both the electrical transport and magnetization are consistent with a Fermi liquid comprised of partially polarized quasiparticle bands. Were $m^*(H, p)$, $\gamma(H, p)$ and

$A(H, p)$ actually to diverge, we would expect $A(H, p)^{-1/2}$ to vanish at H_c and p_c [2]. Instead, $A^{-1/2} \propto T^*$ can be seen to vary in an approximately linear fashion with H and p , intercepting $H = H_c$ and $p = p_c$ at a finite value in both Figs. 2a and b.

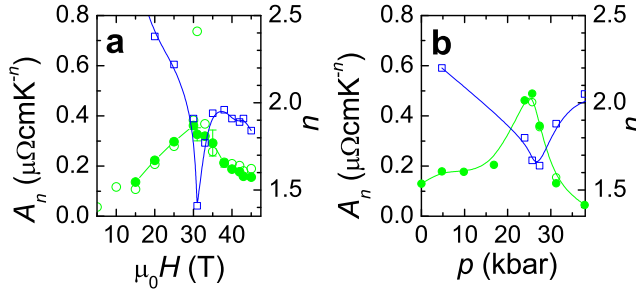


FIG. 4: Coefficient A for $\text{CeIn}_{3-x}\text{Sn}_x$ estimated from $\partial\rho(T)/\partial T$. (a) shows A (filled green circles) estimated as a function of H for $x = 0.25$ and $n = 2$ with open circles showing estimates of A_n where n (open blue squares) is allowed to vary in order to facilitate a comparison with similar measurements under p . Spline fits are drawn to guide the eye. (b) shows similar A data for $x = 0$ as a function of p obtained by Knebel *et al.* [12].

Taken together, these findings imply that the quantum fluctuations of Ψ have a similarly weak effect on the Fermi liquid properties at both p_c in pure CeIn_3 and H_c in $\text{CeIn}_{2.75}\text{Sn}_{0.25}$. Hence, while $\text{CeCu}_{6-x}\text{Au}_x$ [3], $\text{YbRh}_2\text{Si}_{2-x}\text{Ge}_x$ [6] and CeRhIn_5 [7] may be considered consistent with the local criticality picture in which the Fermi surface topology undergoes a dramatic change at the QCP [3], this clearly cannot be the case for CeIn_3 and $\text{CeIn}_{2.75}\text{Sn}_{0.25}$.

One unique advantage of the present H -tuned QCP is that the slope of the phase boundary as $T_N \rightarrow 0$ in Fig. 2 is sufficiently gradual as a function of H that we can continue to observe the proportionality between $A^{-1/2}$, T^* and χ'^{-1} over a significant ~ 12 T wide interval in field below H_c . This continues until $A^{-1/2}(H)$ (rescaled in units of kelvin) intersects $T_N(H)$, whereupon they diverge. The coincidence of the minimum in $A(H)^{-1/2}$ (or maximum in A) at $\mu_0 H_x = 30 \pm 1$ T with the point on the phase diagram at which $T_N \approx T^*$ in Fig. 1b is strongly suggestive of its association with a crossover from SDW-like behavior to local moment-like behavior of the form depicted in Fig. 1b. Such a crossover would directly affect the degree to which the f -electrons contribute charge degrees of freedom to the Fermi liquid [4].

Outside the antiferromagnetic phase, the f -electrons are hybridized with the conduction electrons giving rise to heavy Fermi liquid composed of renormalised quasiparticle bands that incorporate the f -electron charge degrees of freedom [21]. The on-site correlations weaken

with increasing g (i.e. p or H), causing $A^{-1/2}$, T^* and χ'^{-1} all to increase. Provided $T_N \ll T^*$, a weak coupling SDW that gaps parts of the Fermi surface can form [2, 9] with no significant change in the overall effect of the correlations on T^* . To compute of the influence of a finite antiferromagnetic order parameter Ψ on the quasiparticle bands, it is necessary to combine the effect of the on-site Kondo interaction with the $\mathbf{K} = \mathbf{Q}$ (\mathbf{Q} is the antiferromagnetic wave vector) Bragg scattering produced by the underlying antiferromagnetic structure.

At the local QCP depicted in Fig. 1a, T^* vanishes precisely at $g = g_c$ because the Kondo screening is suppressed by the magnetic interactions. The Fermi surface undergoes a large reconstruction across the QCP since the development of antiferromagnetism inhibits the f -electrons from contributing charge degrees of freedom to the Fermi liquid [2, 3], possibly leading to the emergence of new Fermi liquid with a different (smaller) Fermi surface topology and a different characteristic $T^{* \prime}$ that now increases with decreasing g [6] (depicted in red in Fig. 1). In the quantum critical SDW scenario depicted in Fig. 1b, however, the Kondo screening is not suppressed at the QCP and the Fermi surface evolves smoothly across the phase transition. Should H_x correspond to g_x in Fig. 1b, the loss in proportionality between $A^{-1/2}$ and $T^{* \prime}$ for $H < H_x$ can be explained as a consequence of the former being determined for $T \ll T_N$ and the latter for $T > T_N$, with the Fermi surface topology being modified by Ψ only in the former case. Note that χ'^{-1} departs from $A^{-1/2}$ more strongly once $H < H_c$, because it now includes the contribution to the susceptibility from the canted ordered moments.

Our ability to infer $H_x \neq H_c$ in the present study stems from the fact that $H_c \partial T_N / \partial H \ll p_c \partial T_N / \partial p$ close to the QCP. More finely p -tuned NQR studies [13] have recently shown that the lowest Fermi liquid temperature (equivalent to T^*) occurs at a pressure that is ≈ 0.75 kbar lower than p_c , suggesting also that $p_x \neq p_c$. This observation combined with the similar values of $A^{-1/2}$ at which $A^{-1/2}(H, p) \propto T^*(H, p)$ intercepts T_N and the similar minimum ~ 1.5 value of the exponent n (blue squares) obtained on fitting $\rho = \rho_0 + A_n T^n$ to the electrical resistivity data in Fig. 4 suggests that the p - and H -dependent QCP's are related. Both p and H lead to a gradual reduction in the size of the staggered moment and monotonic increase in T^* as the effect of the on-site correlations is suppressed. In the former case this is caused by an increase overlap between the f -electron orbitals while in the latter case it is caused by the progressive polarization of the f -electrons by the Zeeman interaction.

The monotonic $M_z(H)$ of $\text{CeIn}_{3-x}\text{Sn}_x$ is yet another quality that can be attributed to its cubic symmetry. Magnetically anisotropic systems, by contrast, sometimes undergo an abrupt increase in the uniform magnetization (i.e. metamagnetism) at a characteristic magnetic field H_m that is unrelated to antiferromagnetism [22]. Sys-

tems that combine both antiferromagnetism and metamagnetism tend to exhibit a more complicated field-dependent behavior. CeRh_2Si_2 [23] and UPd_2Al_3 [24] are two examples of systems in which metamagnetism causes antiferromagnetism to terminate prematurely at H_m owing to the fact that M_z and Ψ compete for the same spin degrees of freedom.

In summary, we find that the light Sn-doping of CeIn_3 facilitates observation of a H -tuned QCP at $H_c = 42 \pm 2$ T, enabling $\rho(T)$ and $C_p(T)$ measurements to be performed in static magnetic fields $\mu_0 H < 45$ T. Neither $A^{-1/2}$, T^* nor χ'^{-1} collapse to zero at the QCP, indicating that the system continues to exhibit conventional Fermi liquid behavior as $\Psi \rightarrow 0$, suggestive of a 3D quantum critical SDW scenario as opposed to a locally critical scenario. We attribute the observation of a minimum in $A^{-1/2}$ at a somewhat lower field $H_x = 30 \pm 1$ T to the fact that the Kondo screening is not suppressed at the QCP. Correspondingly, T^* continues decreasing until it crosses the antiferromagnetic phase boundary ($T^* = T_N$). At that point, T^* , now T'^* , starts to increase because the order parameter Ψ becomes stronger when the magnetic field is reduced Fig. 1b. A bigger value of Ψ leads to a weaker effective Kondo coupling between the f - and the conduction electrons. Similarities in the electrical transport behavior of $\text{CeIn}_{2.75}\text{Sn}_{0.25}$ at $H_x < H_c$ and CeIn_3 at $p_x < p_c$ [13] suggests that a similar QCP may be accessed in both cases.

The possibility of universality in the H - and p -induced behavior warrants further investigations of pure CeIn_3 by means of electrical transport measurements under combined high H and p conditions. Realization of a situation in which the maximum in m^* and antiferromagnetic QCP occur at distinctly different pressures in CeIn_3 (i.e. $p_x \neq p_c$ in Fig. 1b) [13] may provide a unique opportunity to identify the key factors required to optimize unconventional superconductivity [10].

This work was performed under the auspices of the National Science Foundation, the Department of Energy (US) and the State of Florida. TE would like to thank the Suzuki Foundation for its support in travel expenses, the Casio Science Promotion foundation for additional financial support and Dr. H. Kitazawa of NIMS, Japan for utilizing his arc furnace. AVS acknowledges Pablo Pedrazzini for useful discussions while VF would like to thank the NHMFL In-House Research Program.

[1] S. Sachdev, *Quantum Phase Transitions* (Cambridge Univ. Press, Cambridge, 1999).

[2] P. Coleman *et al.*, *J. Phys.: Condens. Matt.* **13**, R723 (2001).

[3] Q. Si *et al.*, *Nature* **413**, 804 (2001).

[4] In the local quantum critical picture, the magnetic interactions suppress the Kondo screening and, correspondingly, the coherence temperature T^* vanishes at the QCP. Since the RKKY mediated antiferromagnetic order competes with the Kondo screening responsible for formation of the heavy Fermi liquid, it is unlikely that a heavy Fermi liquid that includes the f -electron charge degrees of freedom can continue to survive inside the antiferromagnetic phase. Decoupling of the f -electron charge degrees of freedom from the Fermi liquid should eventually lead to local moment ordering and development of a weakly correlated Fermi liquid with a higher Fermi temperature.

[5] A. Schröder *et al.*, *Phys. Rev. Lett.* **80**, 5623 (1998); O. Stockert *et al.*, *Phys. Rev. Lett.* **80**, 5627 (1998); K. Heuser *et al.*, *Phys. Rev. B* **57**, R4198 (1998).

[6] J. Custers *et al.*, *Nature* **424**, 524 (2003); S. Paschen *et al.*, *Nature* **432**, 881 (2004).

[7] p -dependent dHvA studies on CeRhIn_5 reveal m^* to exhibit a pronounced maximum and the Fermi surface topology to gain ≈ 1 f -electron on suppressing antiferromagnetism with p , both of which are consistent with a local QCP; H. Shishido *et al.*, *J. Phys. Soc. Japan* **74**, 1103 (2005).

[8] J. Lawrence & S. M. Shapiro, *Phys. Rev. B* **22**, 4379 (1980).

[9] T. Moriya, *Phys. Rev. Lett.* **24** 1433 (1970); J. A. Hertz, *Phys. Rev. B* **14**, 1165 (1976); A. J. Millis, *Phys. Rev. B* **48**, 7183 (1993).

[10] N. D. Mathur *et al.*, *Nature* **394**, 39 (1998).

[11] T. Ebihara *et al.*, *Phys. Rev. Lett.* **93**, 246401 (2004).

[12] G. Knebel *et al.*, *Phys. Rev. B* **65**, 024425 (2001).

[13] S. Kawasaki *et al.*, *J. Phys. Soc. Japan* **73**, 1647 (2004).

[14] P. Pedrazzini *et al.*, *Physica B* **312-313**, 406 (2002).

[15] An unidentified phase appears for $x \gtrsim 0.3$, possibly involving an x -induced closure of the gap between the Γ_7 and Γ_8 crystal electric field levels [14].

[16] J. Lawrence, *Phys. Rev. B* **20**, 3770 (1979).

[17] M. Endo *et al.*, *Phys. Rev. Lett.* **93**, 247003 (2004).

[18] H orientation-dependent dHvA experiments performed on pure CeIn_3 at ambient pressure inside the antiferromagnetic phase indicate that m^* increases as $H \rightarrow H_c$ at ‘hot spots’ that occupy $\lesssim 2\%$ of the spherical d-sheet Fermi surface area [11], possibly contributing to the H - and p -dependences of A inside the AFM phase in Figs. 2 a and b.

[19] K. Kadowaki and S. Woods, *Solid State Commun.* **58**, 507 (1986).

[20] K. H. Kim *et al.*, *Phys. Rev. Lett.* **91**, 256401 (2003); K. H. Kim, *et al.* *Phys. Rev. Lett.* **93**, 206401/1-4 (2004).

[21] A. C. Hewson, *The Kondo Problem to Heavy Fermions*, (Cambridge University Press, 1993).

[22] J. Flouquet *et al.*, *Physica B* **319**, 251 (2002).

[23] At ambient pressure, metamagnetism at H_c coincides with H_m , while under high pressures, metamagnetism occurs in the absence of magnetic ordering; T. Hamamoto *et al.*, *Physica B* **281-282** 64 (2000).

[24] T. Terashima *et al.* *Phys. Rev. B* **55**, 13369 (1997).